

Thin Colloidal Crystals

Pawel Pieranski, L. Strzelecki, and B. Pansu

Faculté des Sciences, Laboratoire de Physique des Solides, Université Paris-Sud, F-91405 Orsay, France

(Received 30 August 1982)

Colloidal crystals, made of large polystyrene particles ($1.1 \mu\text{m}$ in diameter), are confined into a thin layer between two glass boundaries. When the thickness h of the layer is increased progressively from zero, a sequence of structures $S(h)$ is detected from direct observations in an optical microscope. These structures are stacks of n square (\square) or triangular (Δ)—ordered layers. For $n \leq 7$, the sequence $S(h)$ is $\dots n\Delta \rightarrow (n+1)\square \rightarrow (n+1)\Delta \rightarrow \dots$.

PACS numbers: 61.50.Cj, 64.70.Kb, 82.70.Kj

Among a large variety of low-dimensional systems we can distinguish one particular class in which the confinement in two (or one) dimensions is achieved by the presence of boundaries. The most common systems possess attractive interactions with surfaces of bulk liquids or solids¹ but repulsive boundaries can also be used for confinement in low dimensions. This latter type of confinement, between two repulsive boundaries, has been proposed and realized experimentally, first by use of macroscopic hard-sphere (or disk) models,² and then by use of colloidal crystals.³

In the geometry of Ref. 3, shown in Fig. 1, the colloidal crystal sample was contained between two solid surfaces—the flat glass plate and the glass sphere. It has been shown³ that thanks to specific interactions of the polymeric colloidal particles with the glass surfaces, perfectly rigid and smooth on the colloidal scale, it is possible to confine a three-dimensional colloidal crystal into a very thin layer.

In the present Letter we report the observation of a series of structural transitions which take place when the thickness h of the colloidal crystal layer (in contact with a three-dimensional reser-

voir) is progressively increased from zero, all other parameters of the system being held constant.

We have chosen for our experiments those colloids made of spherical polystyrene particles, $1.1 \mu\text{m}$ in diameter (D), dispersed in water. The concentrations of particles $N_\infty^{(3)}$ and of the ionic impurities were adjusted for crystallization of bulk samples. Typically, the samples of concentrations 0.12×10^{12} and 0.45×10^{12} (particles/cm³), referred to as samples A and B, have crystallized when the concentration of stray ions was lowered to about 10^{-5} M/l by a purification procedure using an ionic-exchange resin.⁴ These samples, crystalline in bulk, were confined into a thin layer using the plane-sphere (Fig. 1; sample A) or plane-plane (Fig. 2; sample B) geometries. Experiments were performed "in time," when the thickness h between two parallel boundaries (such as in the center of Fig. 1) was increased progressively, or "in space," when the variation of the distance h between the boundaries

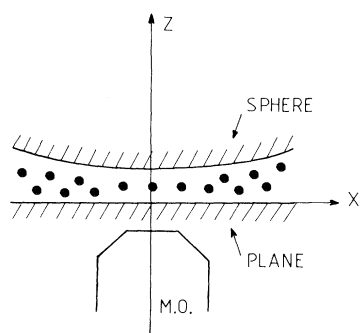


FIG. 1. Schematic of the experimental setup. Plane-sphere geometry of Ref. 3. M.O., microscope objective.

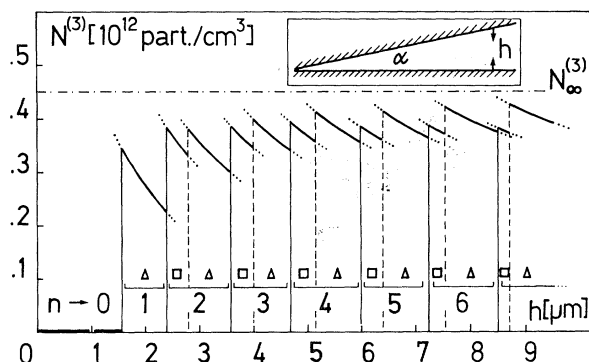


FIG. 2. Plot of the three-dimensional density of particles $N^{(3)}$ as a function of the gap thickness h (sample B, see text). Inset: the plane-plane wedge geometry. $N_\infty^{(3)}$ is the density of an fcc crystal in three dimensions.

is obtained by use of two glass plates forming an angle α (Fig. 2) of about 10^{-2} rad. This last method enables us to visualize directly and simultaneously the structural transitions, which stand out like landmarks, of the passage from two to three dimensions. The observations were made by means of an inverted metallurgical microscope operating either with a high-power objective and in reflected-light illumination mode or with a low-aperture objective and in transmitted-light illumination mode.

With use of this latter method of observation, the typical colloidal crystal sample (B), confined in the plane-plane geometry, appeared as a "patchwork" of distinct, parallel bands of different colors, which (when examined under the high magnification) were found to have different microscopic structures S .⁵ The positions of these bands in the wedge were clearly correlated to the local thickness h so that it became clear that (for a given sample) there exists a series, $S(h)$, characteristic of the passage between two and three dimensions. Among different structures S , those with large width Δh (the interval of the thickness h in which a given structure exists) have been identified as stacks of n two-dimensional crystalline layers with triangular (Δ) or square (\square) intraplanar orders. For increasing thickness h , the following sequence of structures has been established:

$$0 \rightarrow 1\Delta \rightarrow 2\square \rightarrow 2\Delta \rightarrow 3\square \rightarrow \dots \\ \rightarrow n\Delta \rightarrow (n+1)\square \rightarrow (n+1)\Delta \rightarrow \dots$$

This principal qualitative result was confirmed with many other samples such as the sample B for which more quantitative measurements have been made (summarized in Fig. 2). With use of high-magnification photographs (such as those in Fig. 3) the best resolution (which allows us to distinguish between particles) was obtained for the limit layer in the vicinity of the bottom glass plate. The two-dimensional density $N^{(2)}$ of particles was measured in this limit layer and, knowing the number of layers n (counted one by one changing the focusing), the three-dimensional density $N^{(3)}$ was calculated according to the definition $N^{(3)} = N^{(2)}(n/h)$ and plotted as a function of h in Fig. 2. In fact, it has been found that in one layer, the particles behave as if they were hard spheres of effective diameter $D^* = 1.47 \mu\text{m}$; for a given structure (let us say 3Δ) there has not been any noticeable variation of $N^{(2)}$ in the interval $\Delta h^{3\Delta}$ (within the accuracy of measurements,

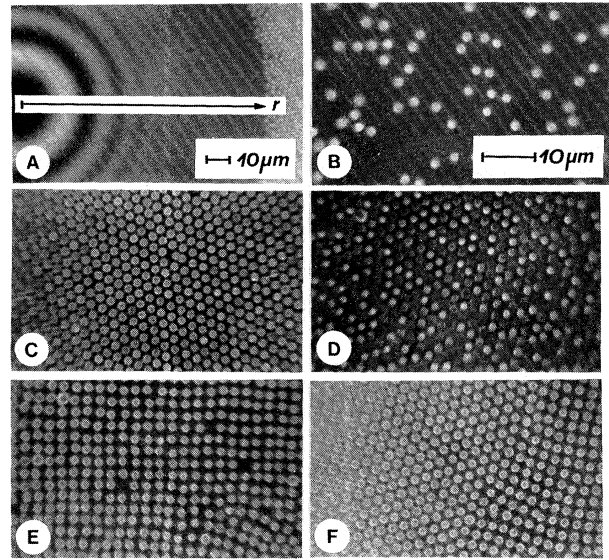


FIG. 3. Photographs illustrating the sequence $S(h)$ of structures characteristic of the passage from two to three dimensions in sample A (see text). The photographs are made with use of the oil-immersion objectives (a) $\times 40$ and (b)–(e) $\times 100$. The diameter of the polystyrene particles is $1.1 \mu\text{m}$. (a) $0 \rightarrow 1$ (formation of the monolayer): The photograph shows an off-center view of the gap. The radius $r_{\text{crit}}^{0 \rightarrow 1}$ of "vacuum" domain defines the critical thickness $h_{\text{crit}}^{0 \rightarrow 1}$. (b) $h > h_{\text{crit}}^{0 \rightarrow 1}$: When the density $N^{(2)}$ of particles is low the monolayer is disordered. (c) $h > h_{\text{crit}}^{1 \rightarrow 1\Delta}$: The monolayer has the triangular intraplanar order. (d) $h > h_{\text{crit}}^{1\Delta \rightarrow 1\Delta e}$: The bright and dark particles are situated at different levels z . The configuration of "up" and "down" particles fluctuates strongly. (e) $h > h_{\text{crit}}^{1\Delta e \rightarrow 2\square}$: The photograph shows one of the square-ordered layers. (f) $2\square \rightarrow 2\Delta$ transition: The thickness of the gap increases from right to left. The transition is obvious.

which is inherently limited by the wedge angle to a few percent) and, on the other hand, the distances between the nearest neighbors in triangular and square layers are almost the same. As a consequence, the variation $N^{(3)}(h)$ shown in Fig. 2 for a given stack of n layers is simply due to the variation of h . In spite of this limitation of accuracy it is clear in Fig. 2 that the alternation of the square and triangular orders allows a better filling of the available space. (A more detailed discussion of arguments for "the best filling of the space" principle is postponed to another article.⁵)

Let us describe now in more detail these structures and the corresponding transitions of the sequence $S(h)$:

$0 \rightarrow (1) \rightarrow 1\Delta$ (*formation of the monolayer*).—This first transition is shown in Fig. 3(a) where the colloidal particles are expelled from the circular region of radius $r_{\text{crit}}^{0 \rightarrow 1}$ (in the plane-sphere geometry). The boundary of the “vacuum” phase, 0, defines the critical thickness $h_{\text{crit}}^{0 \rightarrow 1} \cong 2.2 \mu\text{m}$. In the more concentrated sample *B*, the critical thickness $h_{\text{crit}}^{0 \rightarrow 1} \cong 1.6 \mu\text{m}$ is smaller (Fig. 2). In both cases $h_{\text{crit}}^{0 \rightarrow 1}$ is larger than the “hard-core” diameter $1.1 \mu\text{m}$, measured by means of electron microscopy. In the plane-plane geometry with the wedge angle $\alpha = 10^{-2}$ rad, the monolayer has a liquidlike structure in a very narrow band adjacent to the vacuum phase. Compared with other structures of the sequence $S(h)$, the width $\Delta h = h^{1 \rightarrow 1\Delta} - h^{0 \rightarrow 1}$ of the disordered monolayer is very small and, therefore, has not been indicated explicitly in Fig. 2.

$1\Delta \rightarrow (1\Delta e) \rightarrow 2\Box \rightarrow 2\Delta$ (*formation of the bilayer*).—The particles in the monolayer are subjected to Brownian motions in both horizontal and vertical (z) directions. Both motions can be detected with the optical microscope. In particular, the vertical fluctuations are visible as variations of the brightness of particles. This effect is shown in Fig. 3(d). More precise observations of these vertical fluctuations indicate, for $h > h_{\text{crit}}^{1\Delta \rightarrow 1\Delta e}$, that their amplitude grows and the probability of finding a particle at a level z shows two maxima for $z = h/2 \pm \epsilon$. This transition, which one could call tentatively “an escape in the third dimension,” is a collective phenomenon and presents a theoretical analogy with the antiferromagnetic Ising model on a triangular lattice. In contrast with other transitions, “escape in the third dimension” does not correspond to any noticeable singularity in the plot $N^{(3)}(h)$ in Fig. 2. Upon a further increase of the thickness h the system develops larger fluctuations; close to another transition, characterized by the critical thickness $h_{\text{crit}}^{1\Delta e \rightarrow 2\Box}$, one observes fluctuating domains made of square-ordered bilayers. Above $h_{\text{crit}}^{1\Delta e \rightarrow 2\Box}$ for $1\Delta e \rightarrow 2\Box$, the structure of the stable bilayer is first square and then, upon another transition, the intraplanar structure changes from this square configuration into the triangular one.

$n\Delta \rightarrow (n+1)\Box \rightarrow (n+1)\Delta$.—Up to $n = 7$, the increase of the number of layers n by 1 is accompanied by a transformation of the intraplanar order from the triangular to the square one. The corresponding transition $n\Delta \rightarrow (n+1)\Box$ is very sharp: In the photographs taken with a low-aperture objective, it corresponds to a very distinct boundary between two adjacent bands of different colors. Al-

so, the density $N^{(3)}(h)$, measured from the high-resolution photographs, shows a steplike increase corresponding to this transition (Fig. 2). The triangular intraplanar order is recovered, for a given n , upon a second transition $(n+1)\Box \rightarrow (n+1)\Delta$, which is not as sharp as the previous one. This second transition is in fact preceded by the appearance of a high density of defects of a specific type, which mediate the transformation from the square order into the triangular one. The width of this pretransitional zone increases with increasing n . On the other hand, the overall width of the square-ordered phase $\Delta h^{n\Box}$ decreases with increasing n and the intermediate $n\Box$ phase disappears above $n = 7$.

In conclusion, the sequence $S(h)$ reported for the first time in this Letter can be considered as only one particular, unidimensional section of a very complex phase diagram in a multidimensional phase space. In fact, the problem of finding such a diagram, with the thickness h as one of the dimensions, has been formulated previously in connection with the mechanical modeling of hard-disk and hard-sphere systems.² In this latter case, the phase space is three dimensional; the reduced pressure $\tilde{p} = p/NkT$, the volume fraction Φ , and the reduced thickness $\tilde{h} = h/D_{\text{hs}}$ are the three dimensions of the phase diagram. In the search for such a phase diagram of a thin layer of hard spheres, a particular, purely geometrical (athermal) problem of the most efficient filling of the available space was considered first.⁵ (The two-dimensional case of hard disks has been considered in Ref. 2.) The alternation of phases with triangular and square intraplanar orders has been found in this limit in agreement with the sequence $S(h)$. It is expected, however, that compared with the athermal system of hard spheres, the phase diagram of the thin colloidal crystals should be more complex because the interparticle interaction potential has a soft-core contribution due to the electrostatic repulsion and van der Waals forces. As a result, in stacks of n triangular layers, for $n > 2$, the different stacking orders (such as *ABC* and *ABA* for $n = 3$) should have different internal energy contributions to the thermodynamic potential. Experimentally, in samples such as *A* or *B*, which are rather dilute and made of large particles, the distinction between domains with different stackings is straightforward because they appear, in low magnifications, as “patches” of different colors. For example, in sample *A* these colors are blue for *ABA* and yellow for *ABC* stackings. Our ob-

servation does not indicate either correlations between stackings and local thickness or any clear preference for the fcc or hcp type of stacking. We conclude therefore that in these samples the interactions are in good approximation those of hard spheres.

It is known, however, that in colloidal crystals, made of small polystyrene particles ($0.1 \mu\text{m}$ in diameter), the interactions with farther neighbors are essential and give preference to the bcc structure in thick samples ($h \rightarrow \infty$). In that case, it will be interesting to determine the surface reconstructions in semi-infinite crystals and, consequently, the sequence $S(h)$ in the limit $h \rightarrow 0$.

The effect of thermal motions on the sequence $S(h)$ deserves particular attention. We have observed, in fact, that the sequence $S(h)$ can be altered by the appearance of liquidlike sections. As in other two-dimensional systems the melting of multilayers ($n\Delta$ or $n\Box$) could be mediated by

defects.

We are grateful to Professor J. Friedel for encouraging this research. The authors are indebted to Piotr Pieranski, F. Rothen, M. Gabay, T. Garel, and A. Bonissant for stimulating conversations and a number of illuminating remarks. We thank A. Saint-Martin for technical assistance.

¹See, for example, J. G. Dash, *Films on Solid Surfaces* (Academic, New York, 1975).

²Piotr Pieranski and J. Finney, *Acta Crystallogr., Sec. A* **35**, 194 (1979); Piotr Pieranski, J. Malecki, and K. Wojciechowski, *Mol. Phys.* **40**, 225 (1980); Piotr Pieranski, private communication.

³Pawel Pieranski, L. Strzelecki, and J. Friedel, *J. Phys. (Paris)* **40**, 853 (1979).

⁴See, for example, K. Ametani and H. Fujita, *Jpn. J. Appl. Phys.* **17**, 17 (1978).

⁵B. Pansu, Pawel Pieranski, and L. Strzelecki, to be published.

Low-Energy Electron-Diffraction Intensity Analysis of a Surface Structure with Three CO Molecules in the Unit Cell, Rh(111)-(2 × 2)-3CO: Compact Adsorption in Simultaneous Bridge and Nonsymmetric Near-Top Sites

M. A. Van Hove, R. J. Koestner, and G. A. Somorjai

Materials and Molecular Research Division, Lawrence Berkeley Laboratory, Berkeley, California 94720, and Department of Chemistry, University of California, Berkeley, California 94720

(Received 21 September 1982)

The first low-energy electron-diffraction intensity analysis of the structure of molecules adsorbed at several different surface sites yields, for the compact Rh(111)-(2 × 2)-3CO structure, symmetric bridge sites and nonsymmetric near-top sites, which are separated by only $\sim 2.85 \text{ \AA}$. CO molecules in near-top sites are shifted sideways by $\sim 0.5 \text{ \AA}$ from ideal top sites, but are tilted by less than 15° from the surface normal. These results support an antiphase domain model of high-coverage CO structures on metal surfaces in general.

PACS numbers: 68.20.+t, 61.14.Fe

High-coverage molecular CO overlayers on single-crystal metal surfaces can yield valuable insights into the relative importance of adsorbate-adsorbate and substrate-adsorbate interactions in determining the adsorption site. This is a subject of active debate.¹⁻³ At high coverage the tendency for CO to occupy high-symmetry sites (top, bridge, or hollow sites) is counteracted by steric effects that prevent molecules from approaching each other too closely. Strong repulsive interactions would force molecules into low-symmetry sites determined by a close-packed hexagonal CO lattice, with a more complex bond-

ing character than at high-symmetry sites and a possible tilting of the CO axis away from the surface normal. Among the many known high-coverage CO overlayer structures,² there is one that is particularly favorable for this first low-energy electron-diffraction intensity analysis to determine bond lengths and bond angles in a complex molecular overlayer structure: Rh(111)-(2 × 2)-3CO has a small unit cell containing only three molecules, which allows both a clear-cut high-resolution electron energy-loss spectroscopy (HRELS) investigation and appropriate low-energy electron-diffraction (LEED) calculations. In

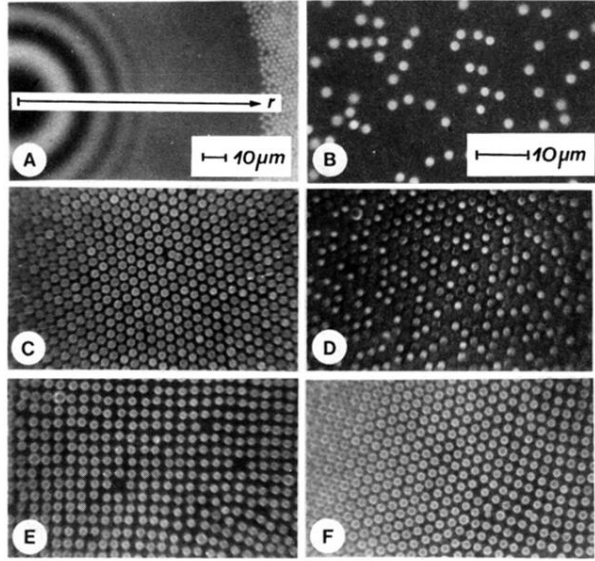


FIG. 3. Photographs illustrating the sequence $S(h)$ of structures characteristic of the passage from two to three dimensions in sample A (see text). The photographs are made with use of the oil-immersion objectives (a) $\times 40$ and (b)–(e) $\times 100$. The diameter of the polystyrene particles is $1.1 \mu\text{m}$. (a) $0 \rightarrow 1$ (formation of the monolayer): The photograph shows an off-center view of the gap. The radius $r_{\text{crit}}^{0 \rightarrow 1}$ of “vacuum” domain defines the critical thickness $h_{\text{crit}}^{0 \rightarrow 1}$. (b) $h > h_{\text{crit}}^{0 \rightarrow 1}$: When the density $N^{(2)}$ of particles is low the monolayer is disordered. (c) $h > h_{\text{crit}}^{1 \rightarrow 1\Delta}$: The monolayer has the triangular intraplanar order. (d) $h > h_{\text{crit}}^{1\Delta \rightarrow 1\Delta e}$: The bright and dark particles are situated at different levels z . The configuration of “up” and “down” particles fluctuates strongly. (e) $h > h_{\text{crit}}^{1\Delta e \rightarrow 2\Box}$: The photograph shows one of the square-ordered layers. (f) $2\Box \rightarrow 2\Delta$ transition: The thickness of the gap increases from right to left. The transition is obvious.